

# Biofabrication, Characterisation and Antimicrobial Activity of CuO/Ag-based Material

Taru Saklani<sup>1</sup> , Naveen Chandra Joshi<sup>2\*</sup>  and Vikash Jakhmola<sup>1</sup> 

<sup>1</sup>Uttaranchal Institute of Pharmaceutical Sciences, Uttaranchal University, Dehradun, Uttarakhand - 248007, India.

<sup>2</sup>Division of Research & Innovation, Uttaranchal University, Dehradun, Uttarakhand - 248007, India.

## Abstract

In this work, *Azadirachta indica* leaf extract and the ultrasonic method were applied for the fabrication of a CuO/Ag-based nanocomposite. The CuO/Ag was characterised using different analytical methods such as FTIR, SEM, EDX, and XRD. The well diffusion method was used to evaluate the antibacterial activity of non-calcined and calcined CuO/Ag against some hazardous bacterial strains. After the incubation period, remarkable zones of inhibition were observed around the loaded CuO/Ag. The maximum zones of inhibition were found to be 17.9 ( $\pm$  0.39), 20 ( $\pm$  0.17), and 14.3 ( $\pm$  0.31) mm for *E. coli*, *S. aureus*, and *S. enterica*, respectively. Experimental findings indicated that non-calcined CuO/Ag was a more effective antibacterial agent as compared to calcined CuO/Ag.

**Keywords:** *Azadirachta indica*, Leaf Extract, CuO/Ag, Antibacterial Activity

\*Correspondence: drnaveen06joshi@gmail.com

**Citation:** Saklani T, Joshi NC, Jakhmola V. Biofabrication, Characterisation and Antimicrobial Activity of CuO/Ag-based Material. J Pure Appl Microbiol. 2024;18(2):1013-1024. doi: 10.22207/JPAM.18.2.16

© The Author(s) 2024. **Open Access.** This article is distributed under the terms of the [Creative Commons Attribution 4.0 International License](https://creativecommons.org/licenses/by/4.0/) which permits unrestricted use, sharing, distribution, and reproduction in any medium, provided you give appropriate credit to the original author(s) and the source, provide a link to the Creative Commons license, and indicate if changes were made.

## INTRODUCTION

Nanotechnology is a discipline of science and technology that focuses on materials with dimensions of less than 100 nm. Nanotechnology has been applied in medicine, energy storage, life sciences, chemical sciences, electronics, and other fields; therefore, industrial sectors are now adopting nanotechnology.<sup>1</sup> There are several types of nanomaterials, comprising carbon-, metal-, organic-, and composite-based nanomaterials.<sup>2</sup> The optical, surface, electrical, and thermal characteristics of metal and metal oxide nanoparticles differ from those of their original bulk materials in a variety of ways.<sup>3</sup> Some typical metal and metal oxide nanoparticles are iron oxides, titania (TiO<sub>2</sub>), copper (Cu), zinc oxide (ZnO), copper oxide (CuO), silver (Ag), and gold (Au). All these nanoparticles possess substantial antibacterial effects against both Gram-negative and Gram-positive bacteria.<sup>4-7</sup> The metal-based nanoparticles provide a viable substitute for conventional antibiotics owing to their diverse physicochemical and functional characteristics and their substantial availability.<sup>8,9</sup> Metal and metal oxide nanoparticles have successfully been produced via the use of biological systems and organic materials in green synthesis, in addition to green chemistry-based methodologies. The green synthesis of metal-based nanoparticles is one of the options that relies on green chemistry concepts and makes use of biological systems. This method is low-cost, effective, and safe.<sup>10,11</sup> Copper oxide nanoparticles (CuO NPs) have received much attention due to their applications in different fields of science and engineering. These nanoparticles are p-type and monoclinic in structure. CuO NPs have been potentially utilised in textiles, biomedicine, sensors, catalysis, water remediation, and high-temperature superconductors.<sup>12-14</sup> Silver nanoparticles (Ag NPs) are extensively used in different industries such as healthcare, food, medicine, cosmetics, energy storage, catalysis, space, and chemical industries due to their unique physical and chemical properties. These include biological characteristics, strong electrical conductivity, optical, electrical, and thermal properties.<sup>15,16</sup> Bhushan *et al.*,<sup>17</sup> used nanoparticles of iron oxide and copper oxide

to produce hybrid magnetic nanocomposites. With a bactericidal efficacy comparable to gentamycin, the nanomaterials demonstrated strong antibacterial activity against harmful bacteria. These non-toxic hybrid nanocomposites possess the potential to be used as antibiotics to treat diseases caused by pathogenic bacteria that are resistant to several drugs. Fe/Ni oxide nanocomposites have been developed by Bhushan *et al.*,<sup>18</sup> who then assessed how effective they were in destroying harmful strains of bacteria. An investigation was conducted on their structural, physical, and chemical characteristics. With the MTT test, their cytotoxicity was evaluated. The study conducted by Bhushan *et al.*,<sup>19</sup> revealed that Fe/Mn oxide nanocomposites were compatible with the MCF7 and MCF-12A cell lines. These nanocomposites possessed outstanding bactericidal activities against various bacteria, such as *Escherichia coli* (*E. coli*), *Bacillus subtilis* (*B. subtilis*), *Staphylococcus aureus* (*S. aureus*), and *Salmonella typhi* (*S. typhi*). It is therefore possible that Fe/Mn oxide nanocomposites will prove to be a viable substitute for conventional antibiotics. Applying the disc diffusion method, Sampath *et al.*,<sup>20</sup> reported the ZnO/Ag nanocomposite's antibacterial activity against *Enterococcus hirae* (*E. hirae*) and *E. coli*. ZnO/Ag nanoparticles showed better antibacterial activity compared to pure ZnO nanoparticles and were found to be stronger than kanamycin. Jaiswal *et al.*,<sup>21</sup> studied the biofabrication of Ag NPs using banana corm extract and silver acetate, achieving MIC values 120, 60, 200, and 100 µg/ml against *E. coli*, *S. aureus*, *Aspergillus brasiliensis* (*A. brasiliensis*), and *Rhizopus stolonifer* (*R. stolonifera*). Through mixing graphitic carbon nitride with CuCl<sub>2</sub>·2H<sub>2</sub>O and NiCl<sub>2</sub>·6H<sub>2</sub>O, Gajurel *et al.*,<sup>22</sup> developed a synergistic bimetallic nano-catalyst that improved catalytic performance in the manufacture of triazole, tetrazole, and bis-triazole derivatives. *Azadirachta indica* is also known as Neem tree. The southern parts of Asia and Africa are where neem trees are most often grown. Consider that the different parts of the Neem tree (bark, fruits, leaves, flowers, gum, and oils) have a long tradition of use in treatments for diseases including diabetes, cancer, heart disease, and hypertension. Due to the presence of some polyphenolic compounds

in the leaves of Neem, these leaves are used as antibacterial, antifungal, and anti-inflammatory agents.<sup>23,24</sup>

## MATERIALS AND METHODS

*Azadirachta indica* leaves, double distilled water (DDW), ethanol, copper acetate [Cu(CH<sub>3</sub>COO)<sub>2</sub>], sodium hydroxide (NaOH), silver nitrate AgNO<sub>3</sub>, and Mueller Hinton agar (MHA) were used in the present work.

### Preparation of extract

After being washed with distilled water, *Azadirachta indica* leaves were allowed to air dry for three to four days. Crushed dry leaves (1 g) were added to 100 ml of DDW. This content was stirred for 25 min and then boiled. 2 ml of 10% ethanol was added to this mixture and shaken for 15 min. The prepared leaf extract was preserved for further study.

### Synthesis of CuO/Ag

2 ml of the extract were combined with 100 mL of a 0.1 M Cu(CH<sub>3</sub>COO)<sub>2</sub> solution. After 35 minutes of shaking, a few drops of 0.1 M NaOH were added. The mixture was stirred for a further 25 min after precipitation. Centrifugation was used to separate the CuO NP precipitate, which was then rinsed and dried. In sealed vials, the non-calcined CuO NPs had been preserved. Calcined CuO NPs were obtained by calcining the dry CuO NPs at 400°C for 2 hr. In 100 ml of a 0.1 M AgNO<sub>3</sub> solution, 2 ml of leaf extract was also added. To produce both non-calcined and calcined Ag NPs, the process described above was repeated. The dry powder of Ag NPs was calcined at 200°C for 2 hr. 50 mg of non-calcined or calcined Ag NPs and 100 mg of non-calcined or calcined CuO NPs in 100 ml of DDW were mixed. The mixture was stirred for 45 min and then sonicated for 3 hr. After complete drying, CuO/Ag (non-calcined or calcined) was preserved for characterization and antibacterial activity. SEM (scanning electron microscopy), EDX (energy dispersive X-ray), FTIR (Fourier transform infrared), and XRD (X-ray diffraction) techniques were used for the characterization of powdered CuO/Ag.

### Antibacterial activity of CuO/Ag

The well diffusion method was used to investigate the antibacterial activity of CuO/Ag against *S. aureus*, *Salmonella enterica* (*S. enterica*), and *E. coli*. 20 ml of liquid MHA was added to sterile petri dishes and allowed to solidify. On the plates, bacterial cultures were spread, and wells were made for the inclusion of CuO/Ag. There were significant zones of inhibition around the CuO/Ag after incubation.

## RESULTS AND DISCUSSION

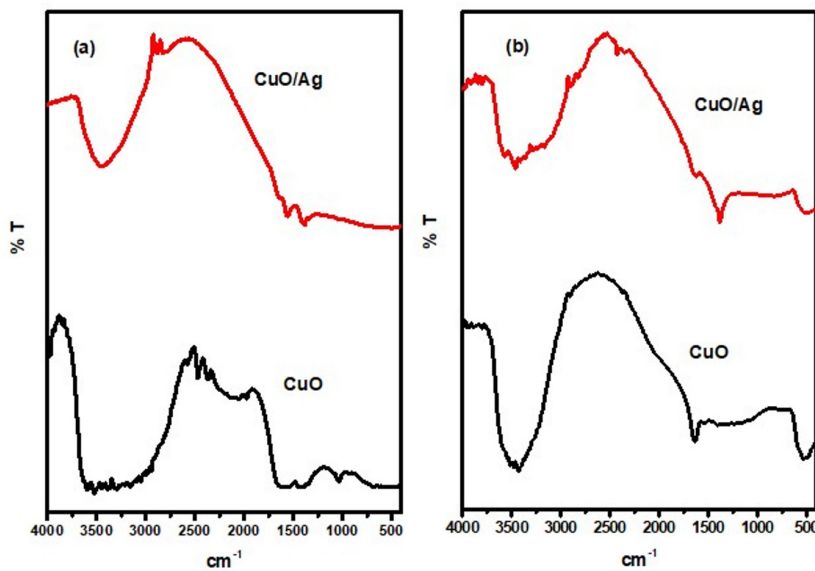
### Characterisation of CuO/Ag

Figure 1(a and b) illustrates the FTIR spectra of non-calcined and calcined CuO/Ag. Non-calcined CuO has distinctive peaks at 3523, 2030, 1620, and 1032 cm<sup>-1</sup> (Figure 1 a). The existence of O-H (str), C=C (allene), O-H (bending), and C-O (asymmetric) bonds is indicated by these peaks. The designated FTIR peaks for non-calcined CuO/Ag are 3455, 1558, 1384, and 531 cm<sup>-1</sup>, respectively. These peaks are associated with bonds like O-H (str), O-H (bending), C-N (str), Cu-O, Cu-Ag, etc.<sup>25-28</sup> The FTIR peaks of 3452, 1627, and 531 cm<sup>-1</sup> have been assigned to calcined CuO and show the presence of O-H (str), O-H (bending), and Cu-O bonds. The FTIR peaks of 3457, 1383, and 506 cm<sup>-1</sup> were also attributed to calcined CuO/Ag. These peaks demonstrate the presence of the O-H (str), C-N (str), and Cu-O or Cu-Ag bonds, respectively.<sup>26-30</sup>

Figure 2 (a and b) presents the XRD patterns of CuO and CuO/Ag. The XRD patterns of non-calcined CuO NPs indicate an amorphous structure and a cluster of peaks due to the presence of different biological constituents of the extract in CuO NPs. A semicrystalline structure of non-calcined CuO/Ag also appears, with peaks that are not related to pure CuO and Ag nanoparticles. For calcined CuO NPs, the XRD peaks have been assigned at 2 θ = 32.5° (110), 35.7° (002), 38.8° (111), 48.9° (202), 53.5° (020), 61.6° (113), 66.3° (311), 68.3° (113), 72.3° (311), and 75.2° (004). These peaks are related to JCPDS card No. 00-041-0254.<sup>21-23</sup> The XRD peaks of CuO/Ag are assigned as 2 θ = 32.6° (110), 35.6° (111), 38.2° (111), 44.4° (200), 48.9° (202), 58.2° (020), 61.6° (113), 64.5°

(220),  $66.3^\circ$  (311),  $68.8^\circ$  (113),  $72.3^\circ$  (311),  $75.2^\circ$  (004), and  $77.4^\circ$  (311), respectively. These all peaks are also satisfying JCPDS card No. 00-041-0254 and JCPDS card No. 04-0783. Based on these patterns, both CuO and CuO/Ag (calcined) phases appear to be crystalline and semi-crystalline. The incorporation of Ag into CuO appears to have affected the crystallinity.<sup>31-37</sup>

The morphological features of CuO NPs and CuO/Ag have been observed using SEM analysis. The SEM images of non-calcined and calcined CuO and CuO/Ag are illustrated in figures 3 and 4. The SEM images of non-calcined CuO indicate the irregular morphology of particles (Figure 3 a and b). Highly agglomerated and irregular-shaped morphology appears in SEM



**Figure 1.** FTIR spectra of (a) non-calcined CuO and CuO/Ag, and (b) calcined CuO and CuO/Ag

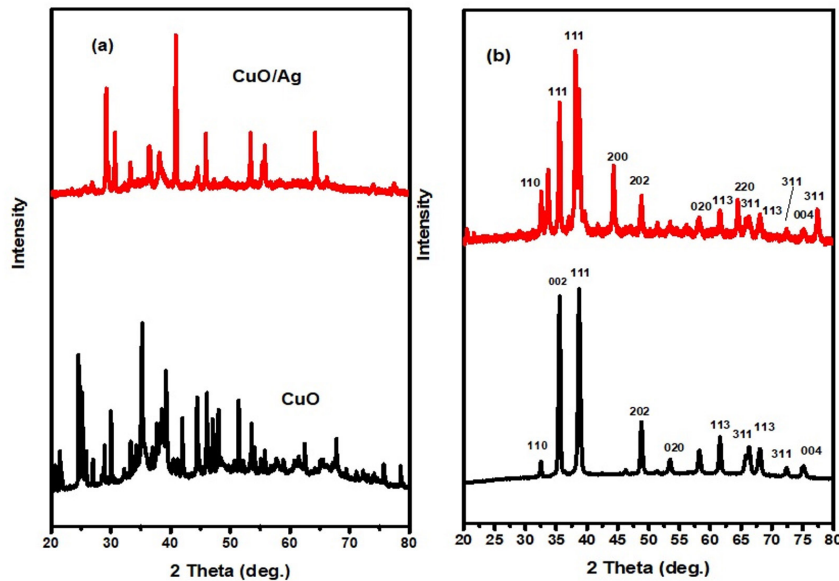


**Figure 2.** XRD patterns of (a) non-calcined CuO and CuO/Ag, and (b) calcined CuO and CuO/Ag

images of non-calcined CuO/Ag (Figure 3 c and d). After calcination, the morphology of CuO appeared to be regular and sphere-shaped (Figure 4 a and b). The morphology of calcined CuO/Ag has been transformed to be less agglomerated and more regular with the combination of sphere- and semi-sphere-shaped particles (Figure 4 c and d). This material is a combination of Ag and CuO that has been heated to eliminate volatile components. Its overall appearance is less agglomerated, more regular, and a mixture of semi-sphere and sphere-shaped particles, indicating that the material has

a range of sizes and orientations. EDX analysis and EDX mapping were used to characterise the elemental composition of the CuO/Ag material. These methods enhance morphological analysis for thorough characterization by offering insights into the material's homogeneity and chemical composition. EDX spectra, composition, and mapping of major elements present in non-calcined and calcined CuO and CuO/Ag are presented in Figures 5 (a and b), 6 and 7, and Tables 1 and 2.

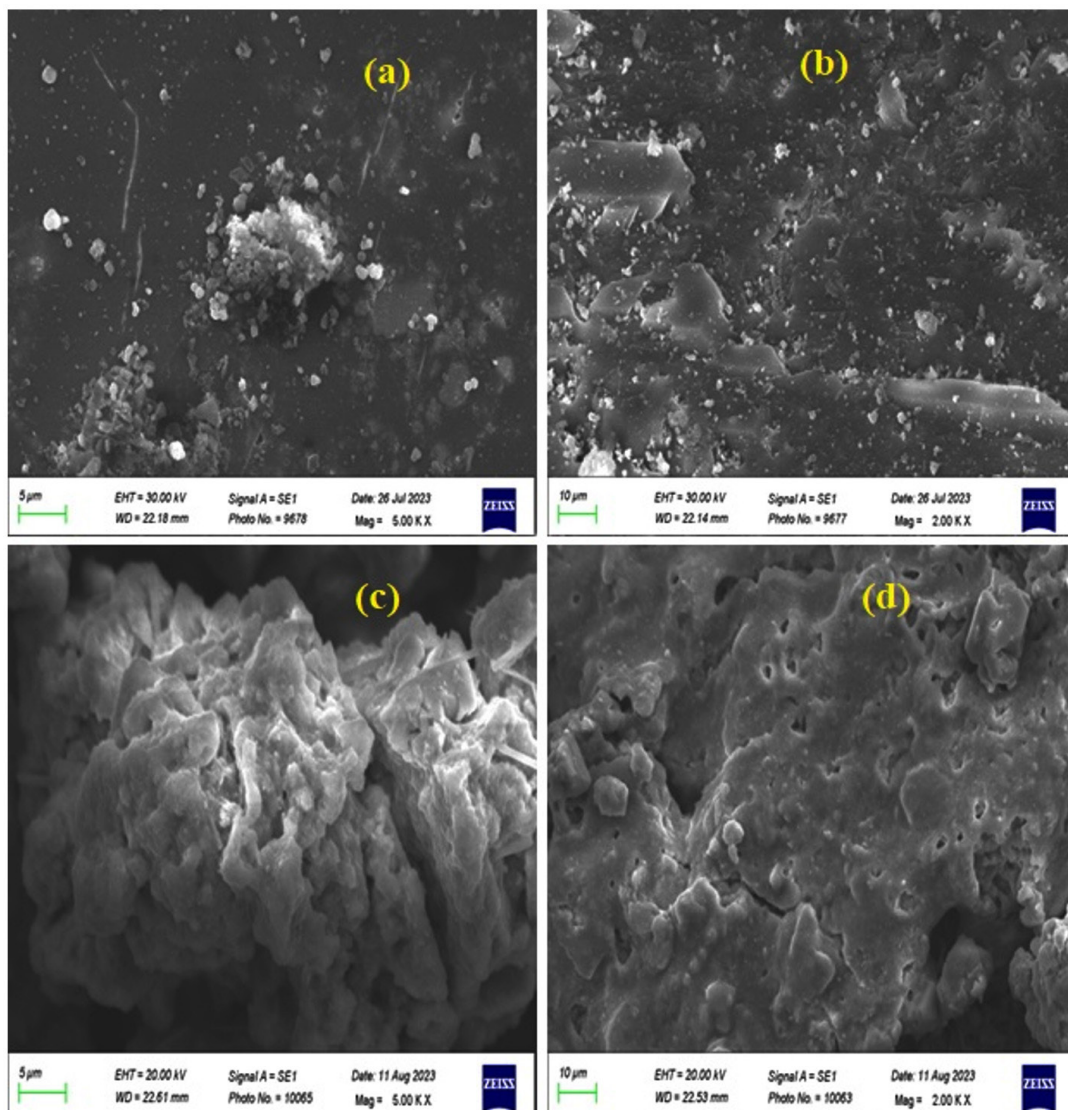


**Figure 3.** SEM images of (a) & (b) non-calcined CuO, and (c) & (d) non-calcined CuO/Ag

### Antibacterial activity of CuO/Ag

Metal and metal oxide nanoparticles have multitarget capabilities that make them potent antibacterial agents.<sup>38</sup> These nanoparticles are capable of distinguishing bacterial cells from mammalian cells.<sup>39</sup> The capability of metal and metal oxide nanoparticles as antibacterial agents has been explained by several mechanisms. Cellular integrity damage, reactive oxygen species (ROS) production, and internalisation of the nanoparticles by the bacterial and fungal cells are a few of these.<sup>40</sup> These nanoparticles generally interact with bacterial membranes, resulting in membrane collapse and rupture, which allows

bacterial cytoplasm to flow out. The oxidative stress caused by the production of reactive oxygen species (ROS) causes the breakdown of bacterial membranes. In general, ROS consists of oxygen, superoxide anion, perhydroxyl radicals, and the hydroxyl radical. These may oxidise proteins and lipids while also damaging DNA and RNA, which causes bacterial death and decomposition.<sup>41</sup> The antibacterial activity of non-calcined CuO/Ag has been conducted using a dosage of 5 to 50 mg/mL. The minimum inhibitory concentration (MIC) was found to be 5 mg/mL. After the incubation period, the zones of inhibition around the non-calcined CuO/Ag were evaluated as  $8 (\pm 0.23)$ ,

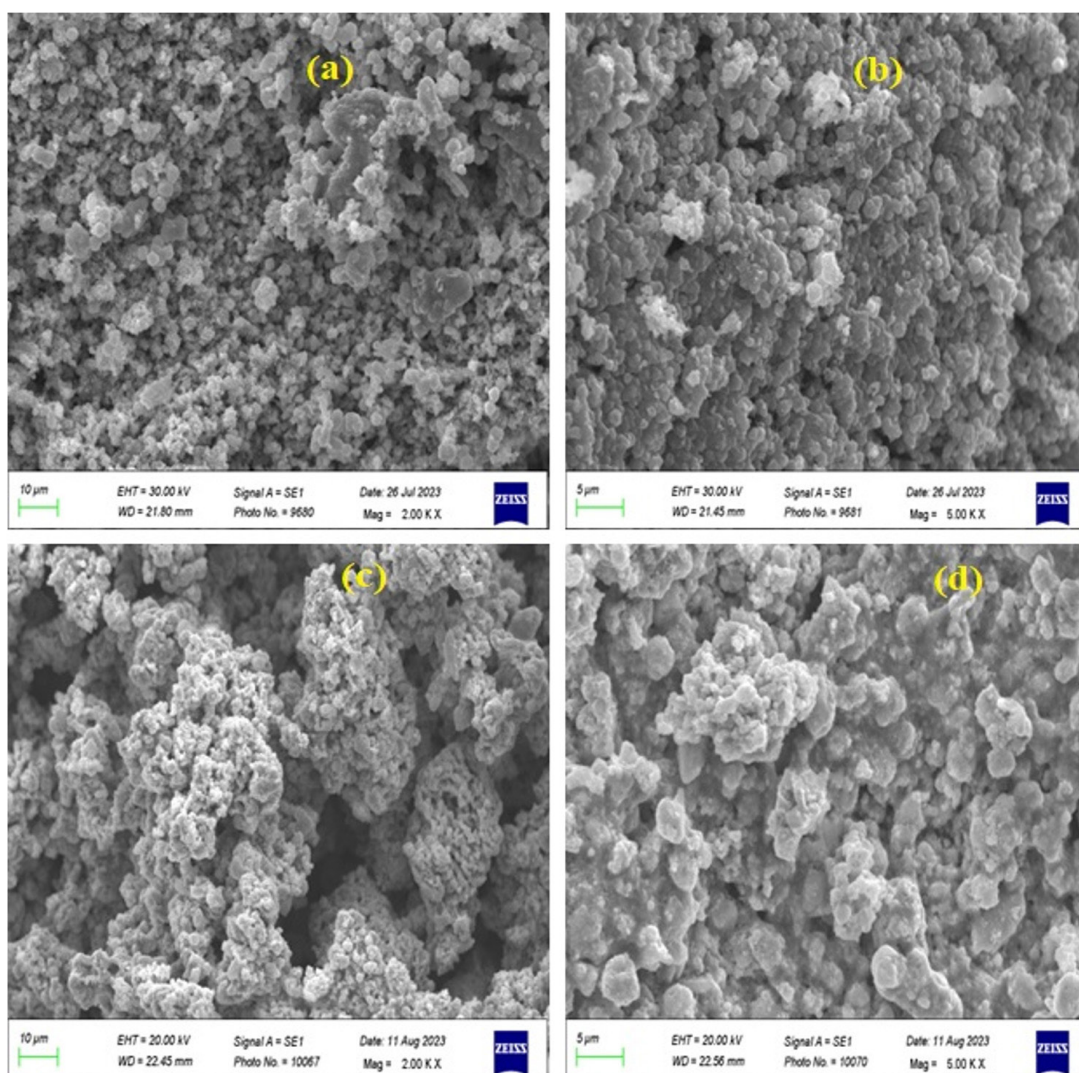


**Figure 4.** SEM images of (a) & (b) calcined CuO, and (c) & (d) calcined CuO/Ag

9.2 ( $\pm$  0.31), and 7.6 ( $\pm$  0.81) mm for *E. coli*, *S. aureus*, and *S. enterica* at an initial dosage of 5 mg/mL. This was increased to 12.6 ( $\pm$  0.69), 12.9 ( $\pm$  0.23), and 9.6 ( $\pm$  0.13) mm at a dosage of 20 mg/L. At 40 mg/mL, the zones of inhibition were found to be 16.7 ( $\pm$  0.17), 17.8 ( $\pm$  0.25), and

13 ( $\pm$  0.51) mm. Then the maximum zones of inhibition were found to be 17.9 ( $\pm$  0.39), 20 ( $\pm$  0.17), and 14.3 ( $\pm$  0.31) mm for *E. coli*, *S. aureus*, and *S. enterica* at 50 mg/mL (Figure 8). The MIC of calcined CuO/Ag was found to be 10 mg/mL. The zones of inhibition for *E. coli*, *S. aureus*, and

**Table 1.** EDX composition of non-calcined CuO/Ag

Element	Weight %	Atomic %
C K	0.6	1.6
O K	40.3	79.6
Cu K	7.7	3.8
Ag L	51.4	15.1

**Table 2.** EDX composition of calcined CuO/Ag

Element	Weight %	Atomic %
O K	12.9	40.8
Cu K	57.1	45.2
Ag L	30.0	14.0

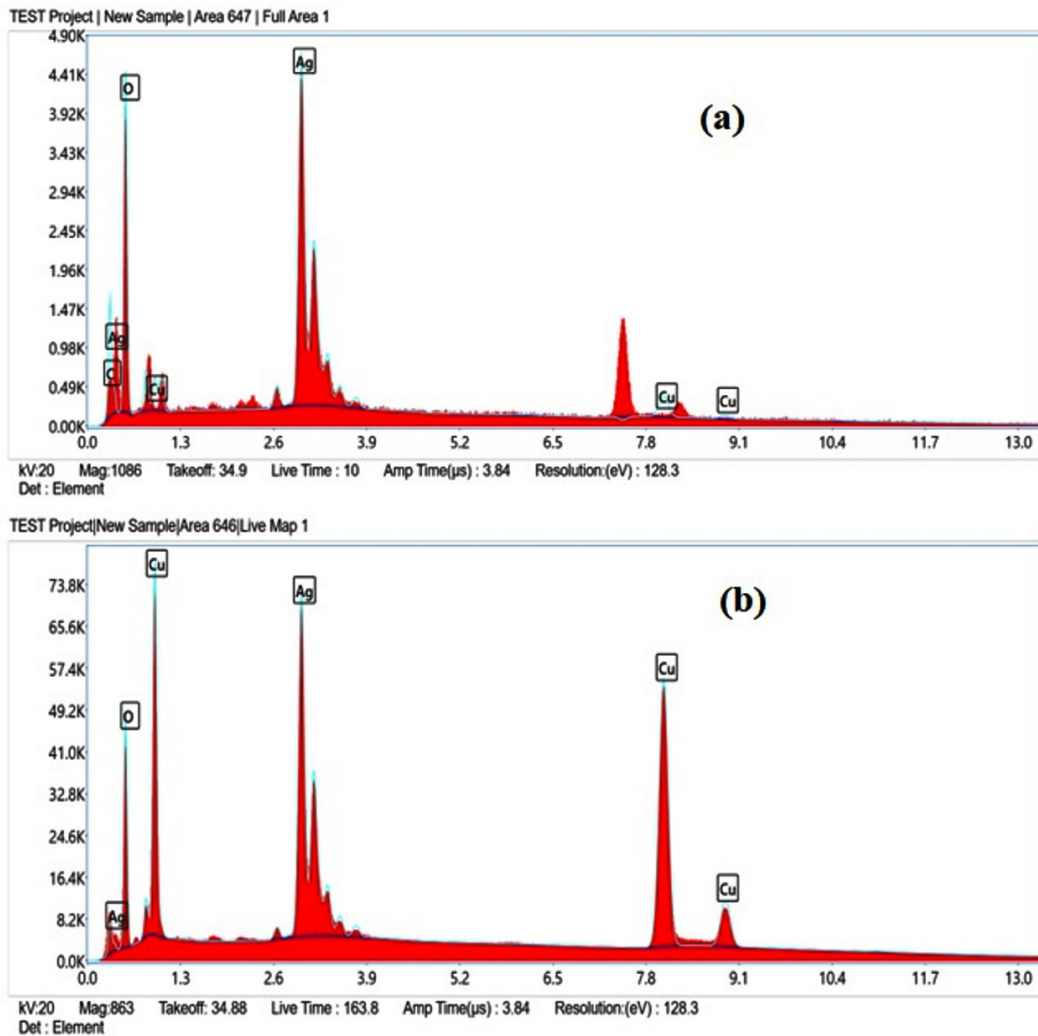


**Figure 5.** EDX spectra of (a) non-calcined CuO/Ag and (b) calcined CuO/Ag

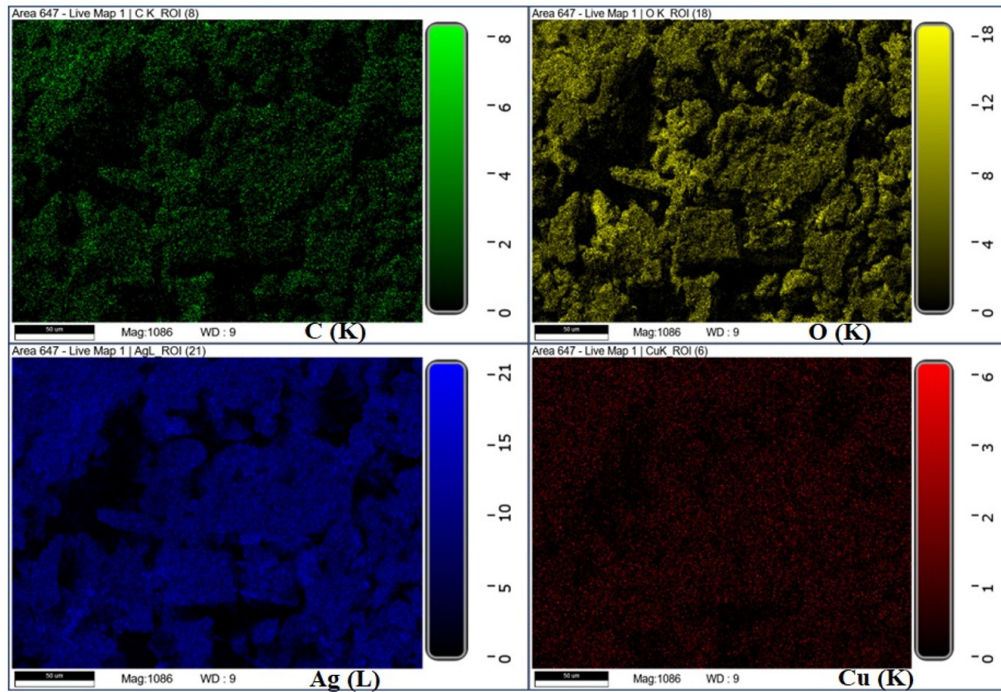


Figure 6. EDX mapping CuO/Ag (non-calcined)

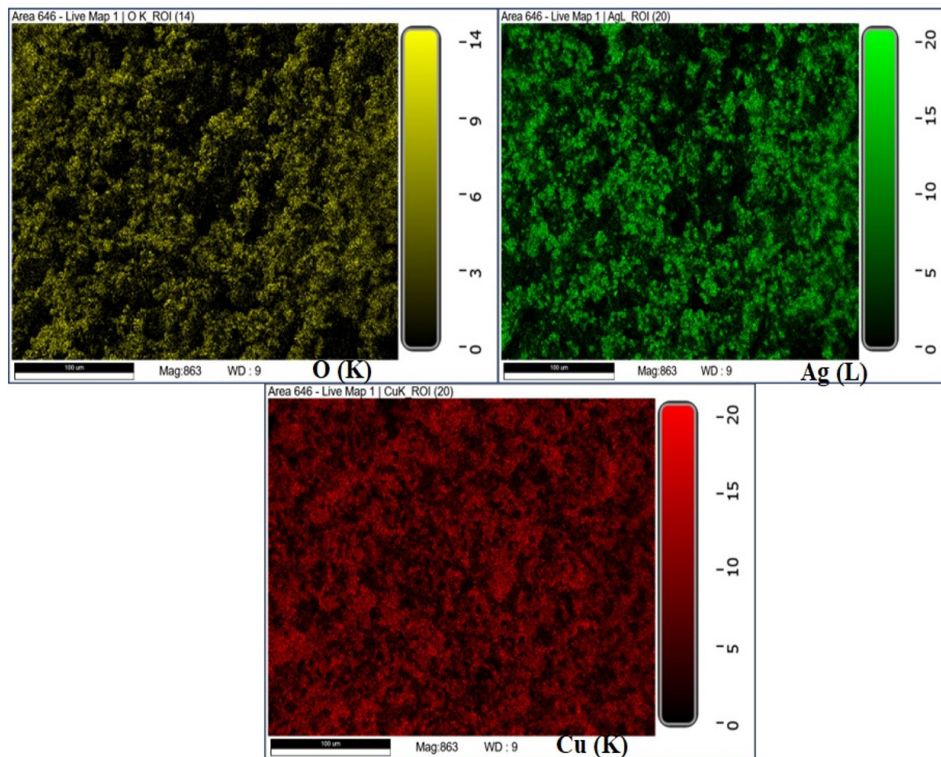


Figure 7. EDX mapping CuO/Ag (calcined)



*S. enterica* were 8.6 mm ( $\pm 0.33$ ), 9.3 mm ( $\pm 0.18$ ), and 7.9 mm ( $\pm 0.25$ ), respectively, at this dose. These values increased to 12.8 mm ( $\pm 0.58$ ), 13.5 mm ( $\pm 0.63$ ), and 9.9 mm ( $\pm 0.37$ ), respectively, at 25 mg/mL. The zones of inhibition were evaluated as 17.8 ( $\pm 0.75$ ), 18.7 ( $\pm 0.89$ ), and 13.2 ( $\pm 0.65$ ) at

50 mg/mL of calcined CuO/Ag. Maximum zones of inhibition were observed as 19.2 ( $\pm 0.25$ ), 20.2 ( $\pm 0.53$ ), and 14.3 ( $\pm 0.36$ ) mm for *E. coli*, *S. aureus*, and *S. enterica* at 60 mg/mL (Figure 9). The experimental findings indicated that non-calcined CuO/Ag was a better antibacterial

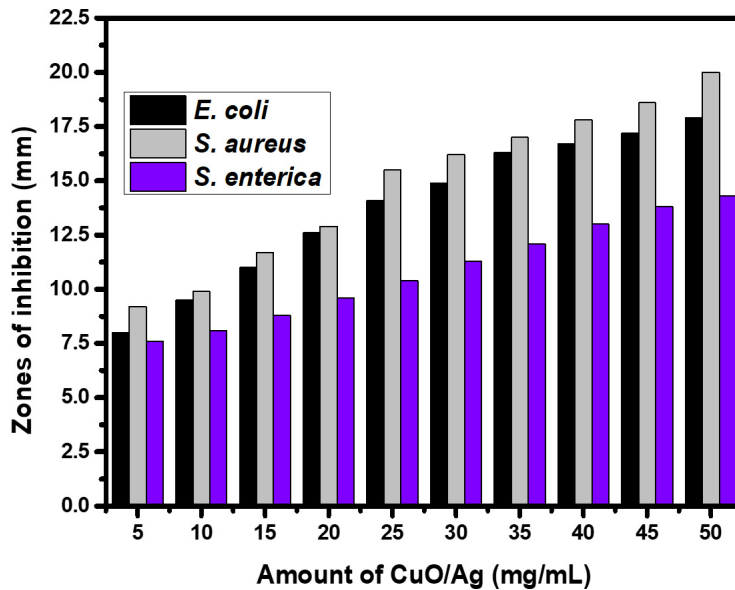


Figure 8. Antibacterial activity of CuO/Ag (non-calcined)

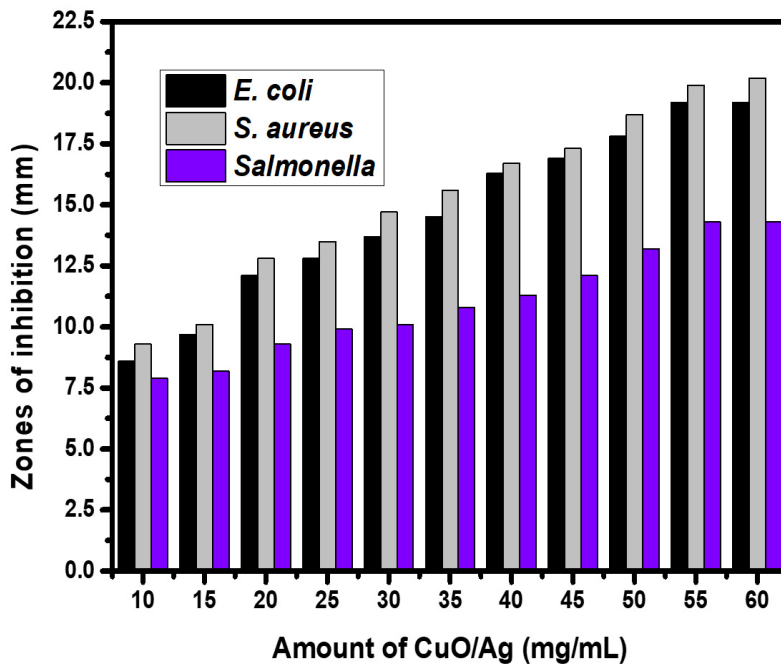


Figure 9. Antibacterial activity of CuO/Ag (calcined)

agent as compared to calcined CuO/Ag. It may be due to the incorporation of biologically active components from the leaf extract into CuO/Ag. After calcination, these components disintegrated and reduced the antibacterial potential of calcined CuO/Ag.<sup>42,43</sup>

## CONCLUSION

*Azadirachta indica* leaf extract and ultrasonication-based synthesis of CuO/Ag were found to be highly efficient, low-cost, and eco-friendly. CuO/Ag has been characterised using different analytical methods. The experimental findings indicated that non-calcined CuO/Ag was a better antibacterial agent as compared to calcined CuO/Ag. At 50 mg/mL of non-calcined CuO/Ag, maximum zones of inhibition around the non-calcined CuO/Ag were found to be 17.9, 20, and 14.3 mm for *E. coli*, *S. aureus*, and *S. enterica* at 50 mg/mL. At the same dosage of calcined CuO/Ag, the zones of inhibition were found to be 17.8, 18.7, and 13.2 mm, respectively.

## ACKNOWLEDGMENTS

The authors are thankful to Uttaranchal University, Dehradun, India, for providing all necessary facilities during the experimental work.

## CONFLICT OF INTEREST

The authors declare that there is no conflict of interest.

## AUTHORS' CONTRIBUTION

All authors listed have made a substantial, direct and intellectual contribution to the work, and approved it for publication.

## FUNDING

None.

## DATA AVAILABILITY

All datasets generated or analyzed during this study are included in the manuscript.

## ETHICS STATEMENT

Not applicable.

## REFERENCES

1. Mody VV, Siwale, Singh A, Mody HR. Introduction to metallic nanoparticles. *J Pharm Bioallied Sci.* 2010;2(4):282-289. doi: 10.4103/0975-7406.72127
2. Sengul AB, Asmatulu E. Toxicity of metal and metal oxide nanoparticles: a review. *Environ Chem Lett.* 2020;18(2):1659-1683. doi: 10.1007/s10311-020-01033-6
3. Rastogi A, Zivcak M, Sytar O, et al. Impact of metal and metal oxide nanoparticles on plant: a critical review. *Front Chem.* 2017;5:78. doi: 10.3389/fchem.2017.00078
4. Dizaj SM, Lotfipour F, Barzegar-Jalali M, Zarrintan MH, Adibkia K. Antimicrobial activity of the metals and metal oxide nanoparticles. *Materials Sci Eng C.* 2014;44:278-284. doi: 10.1016/j.msec.2014.08.031
5. Gudkov SV, Burmistrov DE, Serov DA, Rebezov MB, Semenova AA, Lisitsyn AB. Do iron oxide nanoparticles have significant antibacterial properties? *Antibiotics.* 2021;10(7):884. doi: 10.3390/antibiotics10070884
6. Bhushan M, Kumar Y, Pathak, Y. (eds) Surface Modification of Nanoparticles for Targeted Drug Delivery. *Springer, Cham.* 2019. doi: 10.1007/978-3-030-06115-9\_8
7. Asem D, Kumari M, Singh LR, Bhushan M. Pesticides: Pollution, risks, and abatement measures. *Emerging Aquatic Contaminants.* 2023;307-326. doi: 10.1016/B978-0-323-96002-1.00014-6
8. Raghunath A, Perumal E. Metal oxide nanoparticles as antimicrobial agents: a promise for the future. *Int J Antimicrob. Agents.* 2017;49(2):137-152. doi: 10.1016/j.ijantimicag.2016.11.011
9. Wani IA, Sadeghi B, Kamara SK, Nagabhushana H, Singh LR, Ghosh M, (eds.), *Advancing Medicine through Nanotechnology and Nanomechanics Applications*, IGI Global: Hershey, PA, USA, 2017; 219–249.
10. Ishak NM, Kamarudin SK, Timmiati SN. Green synthesis of metal and metal oxide nanoparticles via plant extracts: an overview. *Mater Res Express.* 2019;6(11):112004. doi: 10.1088/2053-1591/ab4458
11. Shafey EIAM. Green synthesis of metal and metal oxide nanoparticles from plant leaf extracts and their applications: A review. *Green Process. Synthesis.* 2020;9:304-339. doi: 10.1515/gps-2020-0031
12. Waris A, Din D, Ali A, et al. A comprehensive review of green synthesis of copper oxide nanoparticles and their diverse biomedical applications. *Inorg Chem Communi.* 2021;123:108369. doi: 10.1016/j.inoche.2020.108369
13. Naz S, Gul A, Zia M, Javed R. Synthesis, biomedical applications, and toxicity of CuO nanoparticles. *Appl Microbiol Biotechnol.* 2023;107(4):1039-1061. doi: 10.1007/s00253-023-12364-z
14. Kumar M, Mohapatra S. Impact of COVID-19 on Emerging Contaminants: One Health Framework for Risk Assessment and Remediation, Springer Nature. 2022.
15. Zahoor M, Nazir N, Iftikhar M, et al. A review

- on silver nanoparticles: Classification, various methods of synthesis, and their potential roles in biomedical applications and water treatment. *Water*. 2021;13(6):2216. doi: 10.3390/w13162216
16. Zhang XF, Liu ZG, Shen W, Gurunathan S. Silver nanoparticles: synthesis, characterization, properties, applications, and therapeutic approaches. *Int J Mol Sci*. 2016;17(9):1534. doi: 10.3390/ijms17091534
17. Bhushan M, Kumar Y, Periyasamy L, Viswanath AK. Study of synthesis, structural, optical and magnetic characterizations of iron/copper oxide nanocomposites: a promising novel inorganic antibiotic. *Mater Sci Engin :C*. 2019;96:66-76. doi: 10.1016/j.msec.2018.11.009
18. Bhushan M, Kumar Y, Periyasamy L, Viswanath AK. Fabrication and a detailed study of antibacterial properties of a-Fe<sub>2</sub>O<sub>3</sub>/NiO nanocomposites along with their structural, optical, thermal, magnetic and cytotoxic features. *Nanotechnology*. 2019;30(18):185101. doi: 10.1088/1361-6528/ab0124
19. Bhushan M, Mohapatra D, Kumar Y, Viswanath AK. Fabrication of novel bioceramic a-Fe<sub>2</sub>O<sub>3</sub>/MnO nanocomposites: study of their structural, magnetic, biocompatibility and antibacterial properties. *Mater Sci Engin :B*. 2021;268:115119. doi: 10.1016/j.mseb.2021.115119
20. Sampath S, Bhushan M, Saxena V, Pandey LM, Singh LR. Green synthesis of Ag doped ZnO nanoparticles: study of their structural, optical, thermal and antibacterial properties. *Mater Techn*. 2022;37(13):2785-2794 doi: 10.1080/10667857.2022.2075307
21. Jaiswal KK, Banerjee I, Dutta S, et al. Microwave-assisted polycrystalline Ag/AgO/AgCl nanocomposites synthesis using banana corm (rhizome of *Musa* sp.) extract: Characterization and antimicrobial studies. *J Ind Eng Chem*. 2022;107:145-154. doi: 10.1016/j.jiec.2021.11.041
22. Gajurel S, Dam B, Bhushan M, Singh LR, Pal AK. CuO-NiO bimetallic nanoparticles supported on graphitic carbon nitride with enhanced catalytic performance for the synthesis of 1, 2, 3 triazoles, bis 1, 2, 3 triazoles, and tetrazoles in parts per million level. *Appl Organomet Chem*. 2022;36(2):e6524. doi: 10.1002/aoc.6524
23. Islas JF, Acosta E, Zuca G, et al. An overview of Neem (*Azadirachta indica*) and its potential impact on health. *J Funct Foods*. 2020;74:104171. doi: 10.1016/j.jff.2020.104171
24. Alzohairy MA. Therapeutics Role of *Azadirachta indica* (neem) and their active constituents in diseases prevention and treatment. *Evid Based Compl Alternat Med*. 2016;7382506. doi: 10.1155/2016/7382506
25. Saif S, Tahir A, Asim T, Chen Y. Plant mediated green synthesis of CuO nanoparticles: comparison of toxicity of engineered and plant mediated CuO nanoparticles towards *Daphnia magna*. *Nanomaterials*. 2016;6(11):205. doi: 10.3390/nano6110205
26. Dehaj MS, Mohiabadi MZ. Experimental study of water-based CuO nanofluid flow in heat pipe solar collector. *J Thermal Analysis Calorim*. 2019;137(1-2):2061-2072. doi: 10.1007/s10973-019-08046-6
27. Khalir WKAWK, Shameli K, Jazayeri SD, Othman NA, Che Jusoh NW, Hassan NM. Biosynthesized silver nanoparticles by aqueous stem extract of *Entada spiralis* and screening of their biomedical activity. *Front Chem*. 2020;8:620. doi: 10.3389/fchem.2020.00620
28. Yang L, May PW, Yin L, Smith JA, Rosser KN. Ultra fine carbon nitride nanocrystals synthesized by laser ablation in liquid solution. *J Nanoparticle Res*. 2007;9(6):1181-1185. doi: 10.1007/s11051-006-9192-4
29. Kumar I, Gangwar C, Yaseen B, Pandey PK, Mishra SK, Naik RM. Kinetic and mechanistic studies of the formation of silver nanoparticles by nicotinamide as a reducing agent. *ACS Omega*. 2022;7(16):13778-13788. doi: 10.1021/acsomega.2c00046
30. Akintelu SA, Folorunso AS. Characterization and antimicrobial investigation of synthesized silver nanoparticles from *Annona muricata* leaf extracts. *J Nanotechnol Nanomed Nanobiotechnol*. 2019;6:1-5. doi: 10.24966/NTMB-2044/100022
31. Zhu D, Wang L, Yu W, Xie H. Intriguingly high thermal conductivity increment for CuO nanowires contained nanofluids with low viscosity. *Sci Rep*. 2018;8(1):5282. doi: 10.1038/s41598-018-23174-z
32. Ahamed M, Alhadlaq HA, Khan MAM, Karuppiah P, Al-Dhabi NA. Synthesis, characterization, and antimicrobial activity of copper oxide nanoparticles. *J Nanomater*. 2014;637858. doi: 10.1155/2014/637858
33. Mobarak MB, Hossain MS, Chowdhury F, Ahmed S. Synthesis and characterization of CuO nanoparticles utilizing waste fish scale and exploitation of XRD peak profile analysis for approximating the structural parameters. *Arabian J Chem*. 2022;15(10):104117. doi: 10.1016/j.arabjc.2022.104117
34. Meng Y. A Sustainable approach to fabricating Ag nanoparticles/PVA hybrid nanofiber and its catalytic activity. *Nanomaterials*. 2015;5(2):1124-1135. doi: 10.3390/nano5021124
35. Govarthanan M, Selvankumar T, Manoharan K, et al. Biosynthesis and characterization of silver nanoparticles using panchakavya, an Indian traditional farming formulating agent. *Intern J Nanomed*. 2014;9:1593-1599. doi: 10.2147/IJN.S58932
36. Corsino DC, Balela MDL. Room temperature sintering of printer silver nanoparticle conductive ink. *IOP Confer Series: Mater Sci Engin*. 2017;264:012020
37. Das B, Dash SK, Mandal D, et al. Green synthesized silver nanoparticles destroy multidrug resistant bacteria via reactive oxygen species mediated membrane damage. *Arabian J Chem*. 2017;10(6):862-876. doi: 10.1016/j.arabjc.2015.08.008
38. Zhang S, Lin L, Huang X, Lu Y, Zheng D, Feng Y. Antimicrobial properties of metal nanoparticles and their oxide materials and their applications in oral biology. *J Nanomater*. 2022;2063265. doi: 10.1155/2022/2063265
39. Gold K, Slay B, Knackstedt M, Gaharwar AK. Antimicrobial activity of metal and metal oxide based nanoparticles. *Advanced Therapeutics*. 2018;1(3):1700033. doi: 10.1002/adtp.201700033
40. Francis DV, Jayakumar MN, Ahmad H, Gokhale T. Antimicrobial activity of biogenic metal oxide nanoparticles and their synergistic effect on clinical

- pathogens. *Int J Mol Sci.* 2023;24(12):9998. doi: 10.3390/ijms24129998
41. Ogunyemi SO, Abdallah Y, Zhang M, et al. Green synthesis of zinc oxide nanoparticles using different plant extracts and their antibacterial activity against *Xanthomonas oryzae* pv. *Oryzae*. *Artif Cells Nanomed Biotechnol.* 2019;47(1):341-352. doi: 10.1080/21691401.2018.1557671
42. Joshi NC, Negi T, Gururani P. Papaya (*Carica papaya*) leaves extract based synthesis, characterizations and antimicrobial activities of CeO<sub>2</sub> nanoparticles (CeO<sub>2</sub> NPs). *Inorg Nano-Metal Chem.* 2023. doi: 10.1080/24701556.2023.2166068
43. Joshi NC, Chaudhary N, Rai N. Medicinal plant leaves extract based synthesis, characterisations and antimicrobial activities of ZrO<sub>2</sub> nanoparticles (ZrO<sub>2</sub> NPs). *BioNanoSci.* 2021;11(2):497-505. doi: 10.1007/s12668-021-00829-2